

Are there two types of pulsars?

I. Contopoulos^{1,2}

¹*Research Center for Astronomy and Applied Mathematics, Academy of Athens, Athens 11527, Greece*

²*National Research Nuclear University, 31 Kashirskoe highway, Moscow 115409, Russia*

Accepted ... Received ...; in original form ...

ABSTRACT

In order to investigate the importance of dissipation in the pulsar magnetosphere we combined Force-Free with Aristotelian Electrodynamics. We obtain solutions that are ideal (non-dissipative) everywhere except in an equatorial current sheet where Poynting flux from both hemispheres converges and is dissipated into particle acceleration and radiation. We obtain significant dissipative losses similar to what is found in global PIC simulations in which particles are provided only on the stellar surface. We conclude that there might indeed exist two types of pulsars, strongly dissipative ones with particle injection only from the stellar surface, and ideal (weakly dissipative) ones with particle injection in the outer magnetosphere and in particular at the Y-point.

Key words: MHD; Pulsars

1 IDEAL FORCE-FREE MAGNETOSPHERES

For several decades, people have studied the pulsar magnetosphere using the formalism of Force-Free Electrodynamics (hereafter FFE). It has been assumed that electric charges are ‘freely’ supplied anywhere they are needed in order to satisfy the force-free condition, namely

$$\rho_e \mathbf{E} + \frac{1}{c} \mathbf{J}_{\text{FFE}} \times \mathbf{B} = 0. \quad (1)$$

In doing so, any electric field component parallel to the magnetic field is shorted out and

$$\mathbf{E} \cdot \mathbf{B} = 0 \quad (2)$$

everywhere in the magnetosphere. Here, $\rho_e \equiv \nabla \cdot \mathbf{E}/4\pi$ and \mathbf{J}_{FFE} are the electric charge and current densities respectively, and c is the speed of light. Eq. (1) together with Maxwell’s equations yields the following expression for the electric current density

$$\mathbf{J}_{\text{FFE}} = \rho_e c \frac{\mathbf{E} \times \mathbf{B}}{B^2} + c \frac{\mathbf{B} \cdot (\nabla \times \mathbf{B}) + \mathbf{E} \cdot (\nabla \times \mathbf{E})}{B^2} \mathbf{B} \quad (3)$$

(Gruzinov 2006). The work of several researchers has shown that the FFE prescription leads to the development of electric current sheets inside which the force-free condition breaks down (Contopoulos et al. 1999; Spitkovsky 2006; Kalapotharakos & Contopoulos 2009). There are ways to numerically treat current sheets as contact discontinuities, and, as a result, numerical FFE solutions show very little magnetospheric dissipation (less than about 10% of the spindown luminosity) which has mostly been attributed to numerical effects. Still, FFE is not a self-consistent description of the pulsar magnetosphere, and this is why several authors opted for other approaches such as resistive (Kalapotharakos et al.

2012; Li et al. 2012), SFE (Strong Field Electrodynamics; Gruzinov 2008), Aristotelian (particles moving at the speed of light and experiencing radiation reaction opposite to their motion; Gruzinov 2013), ‘ab initio’ global PIC (Particle-In-Cell) simulations, etc. It is interesting to notice that PIC simulations with copious particle injection mimicking pair formation everywhere show little magnetospheric dissipation consistent with ideal FFE (e.g. Philippov & Spitkovsky 2014; Cerutti et al. 2016). On the other hand, PIC simulations with particle injection only from the stellar surface show higher amounts of magnetospheric dissipation (Chen & Beloborodov 2014; Philippov et al. 2015).

We believe that the latter result is physical and not a numerical artifact, and in fact, the goal of the present work is precisely to help us understand whether indeed pulsar magnetospheres fall into two categories, weakly and strongly dissipative ones. Before we proceed, we would like to remind the reader how FFE is implemented numerically. Eq. (3) can be rewritten as

$$\mathbf{J}_{\text{FFE}} = \rho_e c \frac{\mathbf{E} \times \mathbf{B}}{B^2} + \frac{\partial}{\partial t} (\mathbf{E} \cdot \mathbf{B}) \frac{\mathbf{B}}{B^2} + (\mathbf{J} \cdot \mathbf{B}) \frac{\mathbf{B}}{B}. \quad (4)$$

The middle term in the r.h.s. of Eq. (4) obviously disappears if Eq. (2) is implemented. The third term is the part of the electric current that guarantees satisfaction of Eq. (2). In practice, we implement the FFE prescription as follows:

- (i) We set $\mathbf{J} = \rho_e c \mathbf{E} \times \mathbf{B}/B^2$. Obviously the electric current component parallel to \mathbf{B} is missing.
- (ii) We use Maxwell’s equations to advance \mathbf{B} and \mathbf{E} to the next time step using the above expression for the electric current.
- (iii) We correct \mathbf{E} by removing from it any nonzero com-

arXiv:1606.00162v1 [astro-ph.HE] 1 Jun 2016

ponent parallel to \mathbf{B} that accumulated during the above step.

Therefore, the implementation of Eq. (2) is a central procedure in all FFE numerical codes. What is not so obvious in the FFE formalism is that we must add one more constraint, namely that

$$(iv) \quad E \leq B. \quad (5)$$

The latter must be imposed to avoid superluminal drift velocities. It does not come about naturally from the FFE equations, but without it the numerical integration encounters regions where B becomes less than E , and then the numerical code crashes.

As is by now well known, when we integrate the FFE equations, current sheets appear in the magnetosphere. These regions are numerically very problematic and every code addresses them in its own way. Our personal experience has taught us that the extra constraint of Eq. (5) is crucial in FFE, and that without it contact discontinuities do not develop. Also, implementing step (iii) above is numerically unstable because it is a condition that is imposed at every point throughout the numerical grid. Different ways to suppress this numerical instability introduce various amounts of numerical dissipation in the equatorial current sheet and the solutions differ. One way to test the numerical code is to compare its results with the few known high-resolution axisymmetric solutions where indeed current sheets appear as mathematical contact discontinuities.

The above treatment of current sheets is code-dependent thus obviously unsatisfactory, and this is one reason why several researchers opted for global PIC simulations. We believe that it is too early for ‘ab initio’ magnetospheric simulations (for an extended presentation of our arguments see Contopoulos 2016), and we decided instead to investigate the potential of more general formalisms that accommodate current sheets self-consistently. In particular, there is no reason to require that $E \leq B$ inside a current sheet. We thus need to consider a formulation that allows for E to surpass B . One promising such alternative is Aristotelian electrodynamics.

2 DISSIPATIVE MAGNETOSPHERES

Aristotelian electrodynamics (hereafter AE; Finkbeiner et al. 1989) assumes that the charged positive and negative particles that fill the magnetosphere move at (in fact almost at) the speed of light with velocities

$$\mathbf{v}^{\pm} = c \frac{\mathbf{E} \times \mathbf{B} \pm (E_0 \mathbf{E} + B_0 \mathbf{B})}{B^2 + E_0^2}, \quad (6)$$

and that force-balance must include the radiation reaction force along and opposite to the direction of the particle velocity. Here, B_0 and E_0 are the magnitudes of the magnetic and electric field in the frame in which the two are parallel to each other and the particles move along them at the speed of light. The expression for the electric current density becomes

$$\mathbf{J}_{\text{AE}} = \frac{\rho_e c \mathbf{E} \times \mathbf{B} + |\rho_e| c (E_0 \mathbf{E} + B_0 \mathbf{B})}{B^2 + E_0^2}. \quad (7)$$

Eq. (7) is not by itself sufficient to solve for the electromagnetic field structure, and one needs to know the sources of the particles that populate the electric current, thus making the problem complicated and not fully constrained. In particular, Andrei Gruzinov who in the past four years has been the main proponent of AE was the first to discuss the significance of the plasma production process in determining the global structure of the magnetosphere (Gruzinov 2013). He argued that, when particles are supplied only on the stellar surface, he obtains solutions with large amounts of dissipation (30–50% of the spindown luminosity). On the contrary, when particles are freely supplied anywhere in the magnetosphere they are needed (as in Philippov & Spitkovsky 2014; Cerutti et al. 2016), the solutions are closer to ideal FFE with small amounts of dissipation (less than about 10% of the spindown luminosity).

We are determined to understand the main difference between the above two classes of solutions. In order to show how AE transforms Poynting flux into particle energy, Gruzinov offered a simple example that does not require the specification of the rate of particle production, his so-called ‘Device’ (Gruzinov 2014). It is interesting that in his example, $\mathbf{E} \perp \mathbf{B}$ everywhere. In particular, $\mathbf{E} \cdot \mathbf{B} = 0$ not only in the FFE zone, but also in the AE dissipative radiation zone. We believe that this is indeed a simple generalization of the FFE current sheet contact discontinuity. We thus decided to follow his lead and implement a prescription where $\mathbf{E} \cdot \mathbf{B} = 0$ *everywhere* in the magnetosphere. In that special case, the AE prescription simplifies considerably since $E_0 = 0$ if $E \leq B$, and $B_0 = 0$ if $E > B$. We have generalized the FFE numerical prescription as follows:

(i) We set $\mathbf{J} = (\rho_e c \mathbf{E} \times \mathbf{B} + |\rho_e| c E_0 \mathbf{E}) / (B^2 + E_0^2)$. Here, E_0 is either zero (if $E \leq B$), or is equal to $(E^2 - B^2)^{1/2}$ if $E > B$. Obviously the electric current component parallel to \mathbf{B} is missing, as was the case in FFE too.

(ii) We use Maxwell’s equations to advance \mathbf{B} and \mathbf{E} to the next time step using the above expression for the electric current.

(iii) We correct \mathbf{E} by removing from it any nonzero $\mathbf{E} \parallel \mathbf{B}$ component that accumulated during the above step.

The implementation of Eq. (2) is thus a central procedure that either yields FFE in regions where $E \leq B$, or transitions to AE in regions where $E > B$. The numerical integration determines self-consistently where the AE dissipative radiation zones will develop. As we will see next, the new solutions are qualitatively similar to our ‘New Standard Magnetosphere’ (Contopoulos et al. 2014), and also to the results of much more complex large scale PIC simulations with pair supply only from the stellar surface.

2.1 Solutions

We integrate the time-dependent Maxwell’s equations with our new prescription for the electric current. The initial configurations are dipolar at various pulsar inclination angles. Our numerical code is written in (r, θ, ϕ) spherical coordinates with 2° resolution in θ , and ϕ , 1 : 1 grid cell aspect ratio in the r and θ directions, and a 5° avoidance grid zone around the rotation axis $\theta = 0$). We acknowledge that these are our first low resolution crude simulations only meant to support our point about the importance of dissipation in

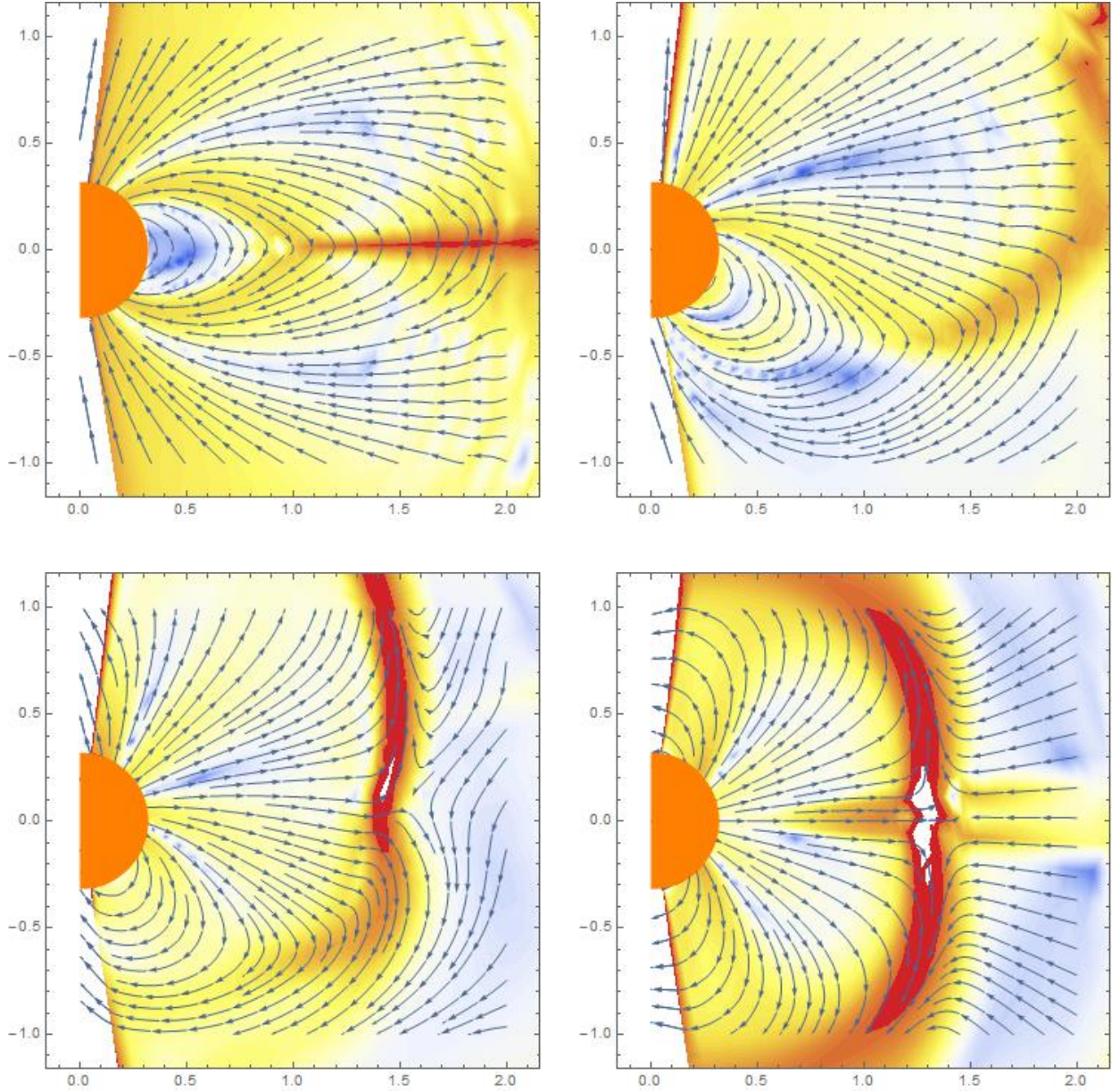


Figure 1. Results of 3D numerical simulations of dissipative magnetospheres after two full rotations for various pulsar inclinations (top left: 0° , top right: 30° , bottom left: 60° , bottom right: 90°). Distances in units of the light cylinder radius. Lines with arrows: magnetic field lines on the poloidal (meridional) plane. Color scale: the magnitude of the poloidal component of $r^2 \nabla \times \mathbf{B}$ (blue: minimum, red: maximum). Red denotes the development of a poloidal current sheet. The current sheet originates at the Y-point and extends outwards.

the pulsar magnetosphere. In Fig. 1 we show the magnetic field and electric current structures on the poloidal plane for various pulsar inclination angles. In all cases, the numerical integration started with a magnetostatic dipole, and then the central ‘star’ was set to uniform rotation. The most important thing to remember is that the new prescription *does not* restrict the magnitude of \mathbf{E} to be less than that of \mathbf{B} . It only requires that the two are everywhere perpendicular to each other.

All solutions shown are strongly dissipative in the equatorial region around the current sheet beyond the light cylinder. It is interesting that the FFE region extends all the way from the axis to the current sheet. There is no transition from FFE to AE at intermediate latitudes as found by Gruzinov. We attribute this difference to our relaxing of the requirement that plasma particles move at the speed of

light everywhere, including the force-free region. In regions where the electric current is timelike, i.e. $J^2 < \rho_e^2 c^2$, eq. (6) does not need to be satisfied.

Another important result is that the current sheet develops *only* in the equatorial region, and does not extend along the boundary of the corotating ‘dead’ zone (the so-called separatrix) to the star. In other words, the separatrix electric current disappears, and only the equatorial current sheet survives. Its electric current consists of the accumulated electric current that flows along the FFE field lines that enter it. It is interesting that this configuration is qualitatively very similar to our ‘New Standard Magnetosphere’ (Contopoulos et al. 2014), in which we had required that the electric current of the equatorial current sheet does not cross the Y-point and continue along the separatrix. We define the Y-point (Y-line in 3D) as the tip of the so called ‘dead’

zone (the corrotating closed line region in which no Poynting flux flows towards the outer magnetosphere). Our main argument in that paper has been that at the Y-point the electric charge density drops to zero, thus if an electric current crossed the Y-point, the current sheet would not be supported electrostatically. Furthermore, in Contopoulos (2016) we argued that it is very hard for particles of the charge type required to support the separatrix current sheet (electrons in the case of aligned pulsars, positrons/protons/ions in the case of counter aligned ones) to cross the Y-point from outside the light cylinder. Our reasoning has been twofold. Firstly, their Speiser orbits are ‘messy’ because when the particles reach the upper and lower outskirts of the current sheet, the overall $\mathbf{E} \times \mathbf{B}$ direction is outwards and not inwards. Secondly, in 3D, the equatorial current sheet outside the light cylinder has an undulating corrotating trailing spiral shape along which particles can only move outwards, not inwards. The above theoretical conclusions seem to be in agreement with the results of global PIC simulations with pair supply only from the stellar surface (Cerutti et al. 2015; Philippov et al. 2015).

Our above arguments for the vanishing of the separatrix electric current sheet *break down* if a) copious pair production at the Y-point supplies the necessary charge carriers to support both the equatorial and separatrix current sheets (as is the case for example in Philippov & Spitkovsky 2014; Cerutti et al. 2016), and b) if a thermal particle population supports the current sheet at the Y-point (see for example Uzdensky & Spitkovsky 2014). The latter possibility seems less likely for relativistic leptons which have radiated away their random motion component. This leads us to agree with Gruzinov (2013) who suggested that there are two types of pulsars, ‘strong’ ones with copious pair production in the outer magnetosphere and in particular at the Y-point, and ‘weak’ ones with particle supply only from the stellar surface. In the latter case, the supplied particles may very well be electrons and protons or ions, which would make aligned weak pulsars very different from counter-aligned weak ones. The latter theoretical conclusion remains to be tested observationally. Notice that, in Gruzinov’s nomenclature, ‘weak’ pulsars are strongly dissipative, and ‘strong’ pulsars weakly!

3 SUMMARY

We have found out that if we combine FFE with AE, a dissipative equatorial current sheet develops beyond the light cylinder in an otherwise ideal pulsar magnetosphere. Poynting flux converges into that region from above and below and is transformed into particle acceleration and radiation, as in Gruzinov’s ‘Device’. The current sheet originates at the Y-point and does not extend along the separatrix to the stellar surface. Its electric current consists of the accumulated electric current that flows along the field lines that enter it. Our solutions are qualitatively similar to our ‘New Standard Magnetosphere’ and may be representative of so-called ‘weak’ pulsars in which particles are supplied only at the stellar surface and not in the outer magnetosphere. They are strongly dissipative, thus very different from the standard ideal FFE weakly dissipative solutions representative of so-called ‘strong’ pulsars in which copious pair production must take place in the outer magnetosphere and in partic-

ular at the Y-point. Intermittent pulsars offer a hint that indeed more than one pulsar configuration may be realized in nature.

Our present numerical simulations do not extend far enough beyond the light cylinder for us to obtain reliable estimates of the amount and distribution of magnetospheric dissipation for various pulsar inclination angles. We plan to obtain more detailed results in a future publication. We believe that we need to invest more effort, both theoretical and numerical, in the investigation of the detailed magnetospheric structure and physical conditions around the Y-point which may hold the key to the determination of the global amount of magnetospheric dissipation.

ACKNOWLEDGEMENTS

We would like to thank the hosts and participants of the 2nd Purdue Workshop on Relativistic Plasma Astrophysics, in particular Drs. Maxim Lyutikov, Andrei Gruzinov, Jonathan Arons, Anatoly Spitkovsky and Alex Chen, who helped us challenge the standard picture of an ideal dissipationless pulsar magnetosphere. Our numerical simulations were performed using the resources of the NRNU MEPhI High-Performance Computing Center.

REFERENCES

- Cerutti B., Philippov A., Parfrey K., Spitkovsky A., 2015, *Mon. Not. Roy. Astron. Soc.*, 448, 606
 Cerutti B., Philippov A. A., Spitkovsky A., 2016, *Mon. Not. Roy. Astron. Soc.*, 457, 2401
 Chen A. Y., Beloborodov A. M., 2014, *Astrophys. J. Lett.*, 795, L22
 Contopoulos I., 2016, *J. Plasma Phys.*, in press
 Contopoulos I., Kazanas D., Fendt C., 1999, *Astrophys. J.*, 511, 351
 Contopoulos I., Kalapotharakos C., Kazanas D., 2014, *Astrophys. J.*, 781, 46
 Finkbeiner B., Herold H., Ertl T., Ruder H., 1989, *Astron. Astrophys.*, 225, 479
 Gruzinov A., 2006, *ArXiv e-prints*, astro-ph/0604364
 Gruzinov A., 2008, *ArXiv e-prints*, 0802.1716
 Gruzinov A., 2013, *ArXiv e-prints*, 1303.4094
 Gruzinov A., 2014, *ArXiv e-prints*, 1402.1520
 Kalapotharakos C., Contopoulos I., 2009, *Astron. Astrophys.*, 496, 495
 Kalapotharakos C., Harding A. K., Kazanas D., Contopoulos I., 2012, *Astrophys. J. Lett.*, 754, L1
 Li J., Spitkovsky A., Tchekhovskoy A., 2012, *Astrophys. J.*, 746, 60
 Philippov A. A., Spitkovsky A., 2014, *Astrophys. J. Lett.*, 785, L33
 Philippov A. A., Spitkovsky A., Cerutti B., 2015, *Astrophys. J. Lett.*, 801, L19
 Spitkovsky A., 2006, *Astrophys. J. Lett.*, 648, L51
 Uzdensky D. A., Spitkovsky A., 2014, *Astrophys. J.*, 780,